nature medicine

SUPPLEMENTARY INFORMATION

https://doi.org/10.1038/s41591-018-0057-z

In the format provided by the authors and unedited.

A transcriptionally and functionally distinct PD-1$^+$ CD8$^+$ T cell pool with predictive potential in non-small-cell lung cancer treated with PD-1 blockade

Daniela S. Thommen[1,2*], Viktor H. Koelzer[3,4,13], Petra Herzig[1,13], Andreas Roller[5,13], Marcel Trefny[1], Sarah Dimeloe[6], Anna Kiialainen[5], Jonathan Hanhart[3], Catherine Schill[7], Christoph Hess[6], Spasenija Savic Prince[8], Mark Wiese[9], Didier Lardinois[9], Ping-Chih Ho[10], Christian Klein[11], Vaios Karanikas[11], Kirsten D. Mertz[3], Ton N. Schumacher[2,14] and Alfred Zippelius[1,12,14*]

[1]Cancer Immunology, Department of Biomedicine, University Hospital Basel, Basel, Switzerland. [2]Division of Molecular Oncology and Immunology, Oncode Institute, The Netherlands Cancer Institute, Amsterdam, The Netherlands. [3]Institute of Pathology, Cantonal Hospital Baselland, Liestal, Switzerland. [4]Molecular and Population Genetics Laboratory, University of Oxford, Oxford, UK. [5]Roche Pharmaceutical Research and Early Development, Roche Innovation Center Basel, Basel, Switzerland. [6]Immunobiology, Department of Biomedicine, University Hospital Basel, Basel, Switzerland. [7]Oncology, Cantonal Hospital Baselland, Liestal, Switzerland. [8]Institute of Pathology, University Hospital Basel, Basel, Switzerland. [9]Department of Surgery, University Hospital Basel, Basel, Switzerland. [10]University of Lausanne, Ludwig Center for Cancer Research, Epalinges, Switzerland. [11]Roche Pharmaceutical Research and Early Development, Roche Innovation Center Zurich, Zurich, Switzerland. [12]Medical Oncology, University Hospital Basel, Basel, Switzerland. [13]These authors contributed equally: Viktor H. Koelzer, Petra Herzig, Andreas Roller. [14]These authors jointly directed this work: Ton N. Schumacher, Alfred Zippelius. *e-mail: d.thommen@nki.nl; alfred.zippelius@usb.ch

Supplementary Figure 1

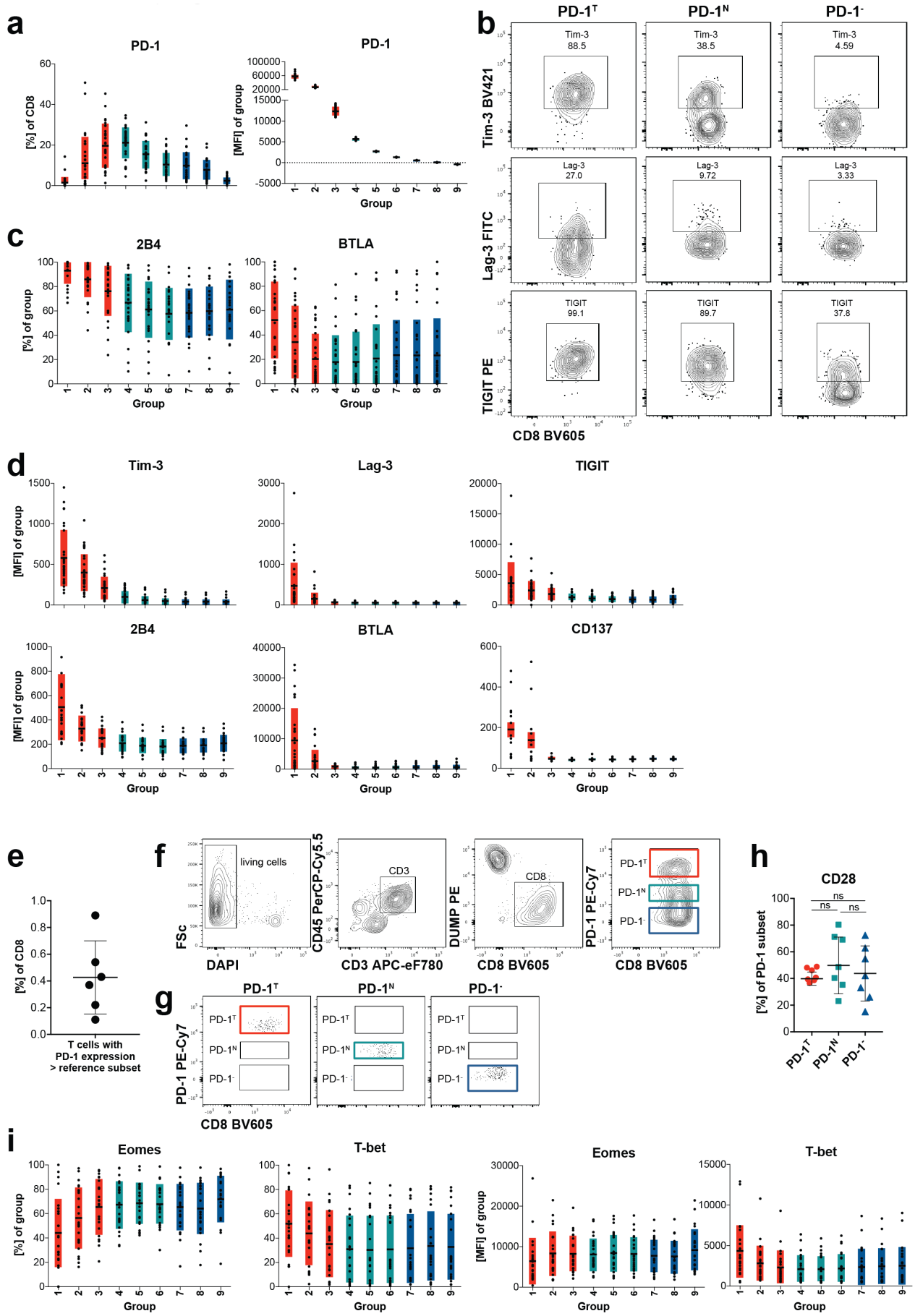

Supplementary Figure 1. Expression of inhibitory and activating receptors correlates with PD-1 level. (**a**) Distribution of $CD8^+$ TILs with different levels of PD-1 expression (n=24). Lines and boxes represent mean and SD, respectively. (**b**) Representative flow cytometry plots depicting staining of Tim-3, Lag-3 and TIGIT on the PD-1 subsets, one exemplary NSCLC specimen is shown (from n=3 independent experiments). (**c+d**) Percentage expression (**c**) and mean fluorescence intensity (**d**) of indicated inhibitory and activating co-receptors on PD-1 subgroups (n=24). Lines and boxes represent mean and SD, respectively. (**e**) Percentage of PD-1 high expressing cells in peripheral blood $CD8^+$ T cells of healthy donors (n=6). Shown are mean and SD. (**f**) Gating strategy and (**g**) post-sort analysis of $PD\text{-}1^T$, $PD\text{-}1^N$ and $PD\text{-}1^-$ $CD8^+$ TIL subsets. (**h**) CD28 expression on PD-1 subsets. Shown are mean and SD. Statistical significance was determined using one-way ANOVA. (**i**) Percentage expression and mean fluorescence intensity of the transcription factors Eomes and T-bet expressed by PD-1 subgroups (n=24). Lines and boxes represent mean and SD, respectively.

Supplementary Figure 2

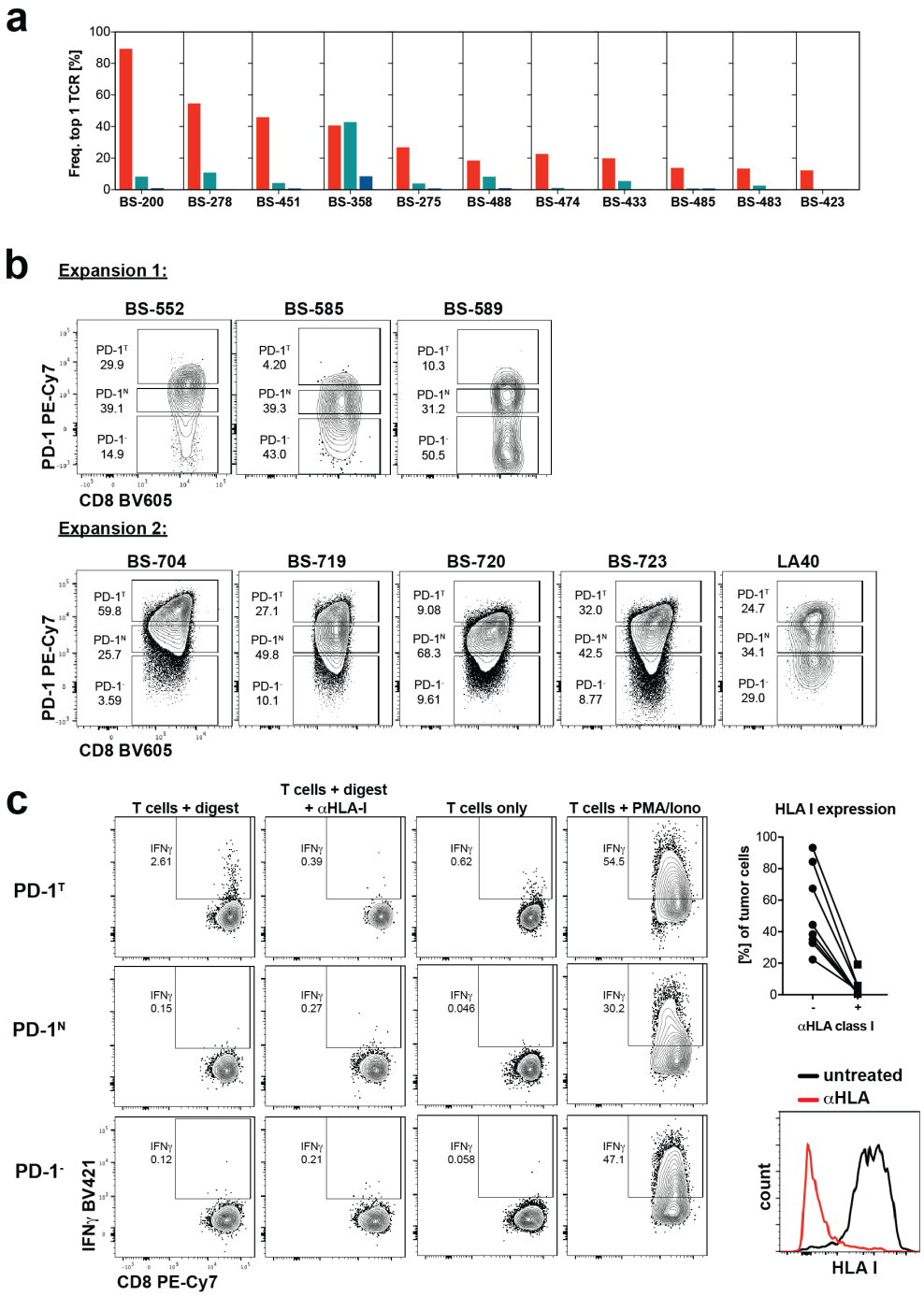

Supplementary Figure 2. PD-1^{T} TILs show enhanced tumor reactivity. (**a**) Frequency of the top 1 TCR clone of PD-1^{T} TILs within all three PD-1 subsets. (**b**) PD-1 expression on CD8^{+} TILs before sorting and expansion of the NSCLC specimens used for tumor reactivity assessment. 'Expansion 1' and 'Expansion 2' reflect two independent sample sets that were sorted and expanded on separate occasions. The PD-1 subsets from the three tumor specimens in expansion 1 were also used for the experiments (PD-1 expression and IFN-γ secretion) in Fig. 1h. (**c**) IFN-γ production of expanded PD-1 subsets of one representative donor upon co-culture with autologous tumor digest. Shown is the difference in IFN-γ secretion in the absence or presence of an HLA class I blocking antibody, as well as controls with T cells only or T cells stimulated with PMA/ionomycin (left part of the figure, from n=3 independent experiments). Percentage of tumor cells with detectable HLA class I staining in the absence or presence of pre-treatment with an HLA class I blocking antibody (right part).

Supplementary Figure 3

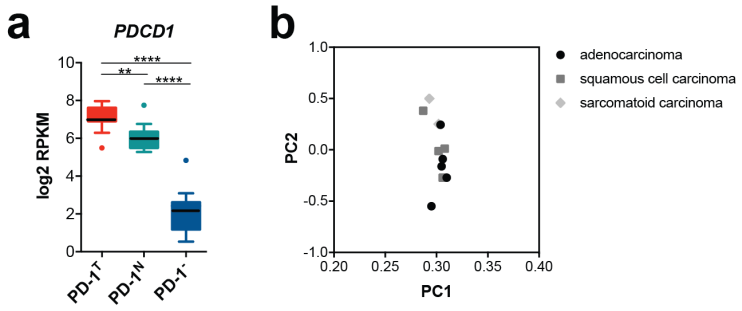

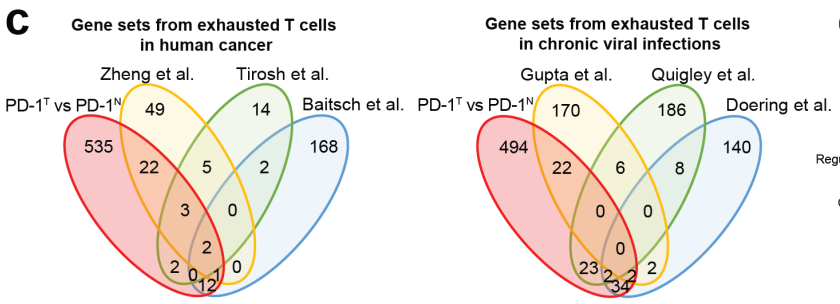

Gene set	Overlap of gene set with PD-1^T signature: % (n of n genes)	T cell signature	Disease	Species	GEO accession number
Zheng et al. 2017	34.1% (28/82)	Single cell sequencing, exhausted vs non-exhausted TILs	HCC	human	GSE98638
Tirosh et al. 2016	25% (7/28)	Single cell sequencing, exhausted CD8$^+$ TIL signature	Melanoma	human	GSE72056
Baitsch et al. 2011	8.1% (15/185)	Melan-A-specific CD8$^+$ T cells from metastases vs blood	Melanoma	human	GSE24536
Gupta et al. 2015	11.9% (24/202)	Antigen-specific CD39$^+$ vs CD39$^-$ CD8+ T cells	HCV	human	GSE72752
Quigley et al. 2010	11.1% (25/225)	HIV-specific CD8$^+$ T cells in progressors	HIV	human	GSE24082
Doering et al. 2012	20.2% (38/184)	Antigen-specific PD-1^{hi} vs PD-1^{int} CD8$^+$ T cells	LCMV clone 13	murine	GSE41869

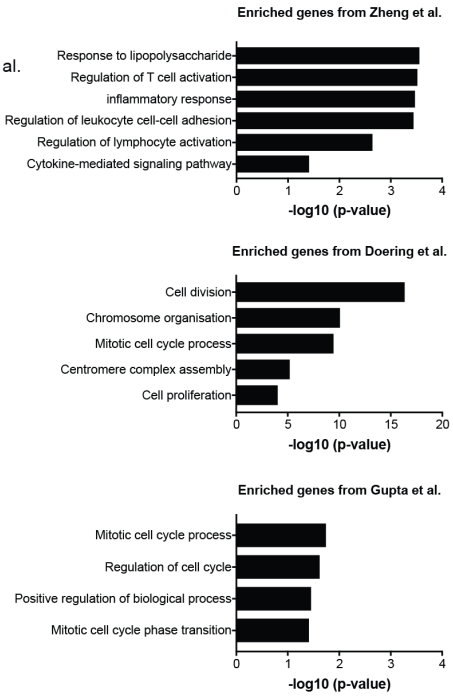

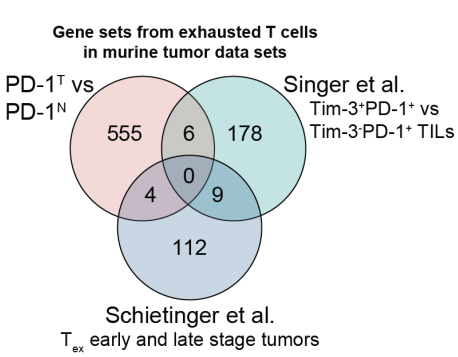

Gene set	Overlap of gene set with PD-1^T signature % (n of n genes)	T cell signature	Disease	Species	GEO accession number
Schietinger et al. 2016	4% (5/125)	Early and late-exhaustion genes	Liver carcinoma	murine	GSE60501
Singer et al. 2017	3.1% (6/193)	Tim-3$^+$PD-1$^+$ vs Tim-3$^-$ PD-1$^+$ TILs	Melanoma	murine	GSE86042

Supplementary Figure 3. Validation of RNA seq data and comparison with other exhaustion data sets. (**a**) *PDCD1* gene expression in sorted PD-1 subsets (n=11). The lines in the box-and whisker-plots indicate median values, the boxes IQR values and the whiskers 1.5IQR values as calculated by Tukey. $^{**}P < 0.01$, $^{****}P < 0.0001$ by one-way ANOVA, (**b**) PCA analysis of the PD-1^T subset with histologic tumor subtypes indicated (n=11). (**c**) Venn diagrams showing the overlap of differentially expressed genes between PD-1^T and PD-1^N TILs and six gene sets with exhaustion signatures derived from T cells in distinct human or murine chronic

viral infections and human cancers. (**d**) Venn diagram showing the overlap of differentially expressed genes between PD-1^T and PD-1^N TILs and two gene sets with exhaustion signatures derived from T cells in murine cancers. (**e**) Biological processes (GO terms) enriched in genes derived from three data sets in (**c**) that overlap with the PD-1^T signature (n=11).

Supplementary Figure 4

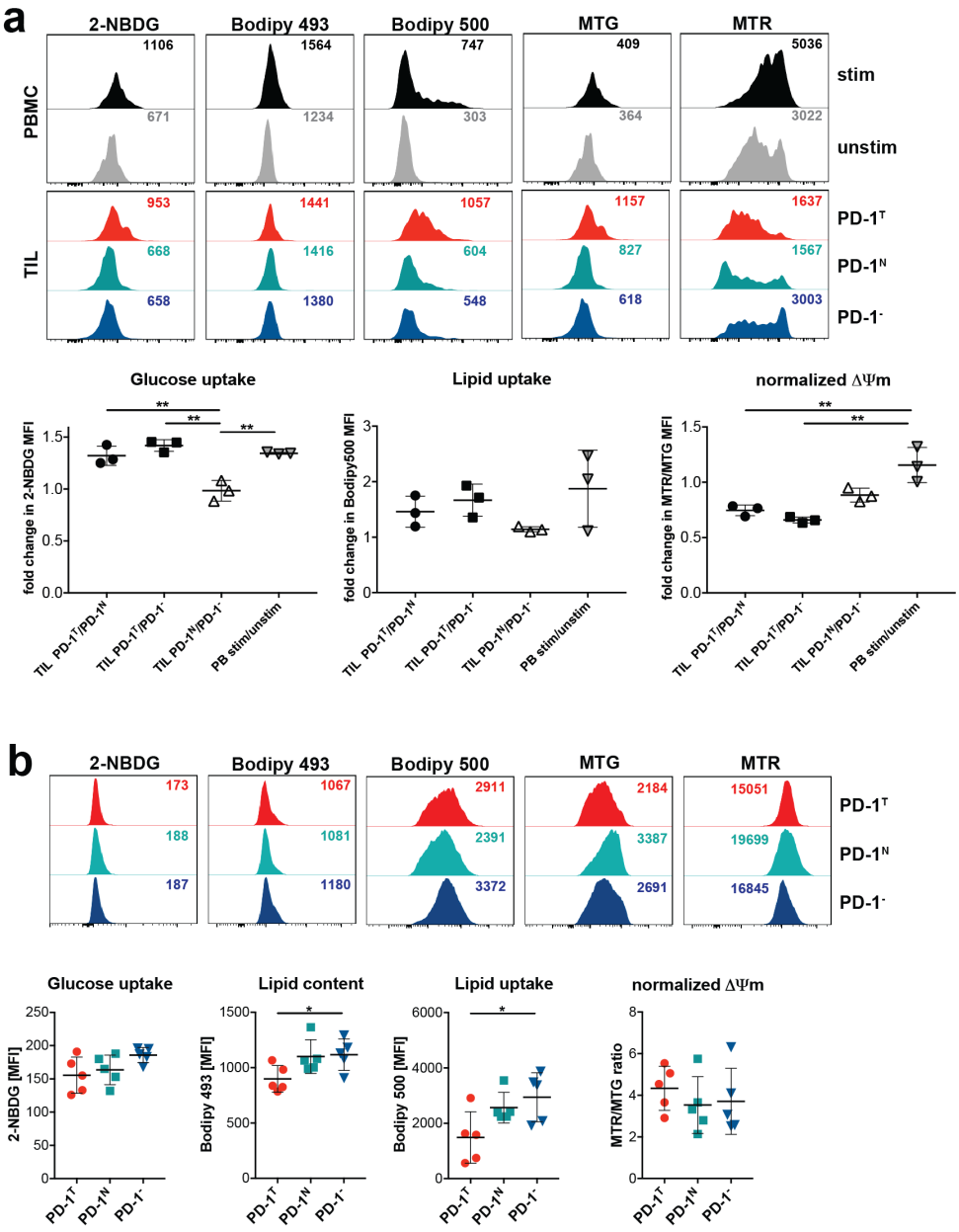

Supplementary Figure 4. Metabolism of peripheral blood T cells and of PD-1 subpopulations upon expansion. (**a**) Changes in glucose and lipid uptake as well as mitochondrial metabolism in peripheral blood $CD8^+$ T cells upon anti-CD3/anti-CD28 stimulation compared to the differences between the PD-1 subsets. Histograms of flow cytometry data of $CD8^+$ T cells from one representative healthy donor and one NSCLC patient and the fold change between the respective PD-1 subsets (n=3) and unstimulated/stimulated peripheral $CD8^+$ T cells (n=3) are depicted. Shown are mean and SD. $^{**}P < 0.01$ by one-way ANOVA. (**b**) Normalization of metabolism in TILs derived from $PD\text{-}1^T$, $PD\text{-}1^N$ and $PD\text{-}1^-$ cells upon expansion in high-dose IL-2. Histograms of flow cytometry data of one representative experiment and the quantification of all NSCLC specimens from expansion 2 (n=5 tumor specimens) are depicted (Supplementary Fig. 2b). Shown are mean and SD. $^{*}P < 0.05$ by one-way ANOVA.

Supplementary Figure 5

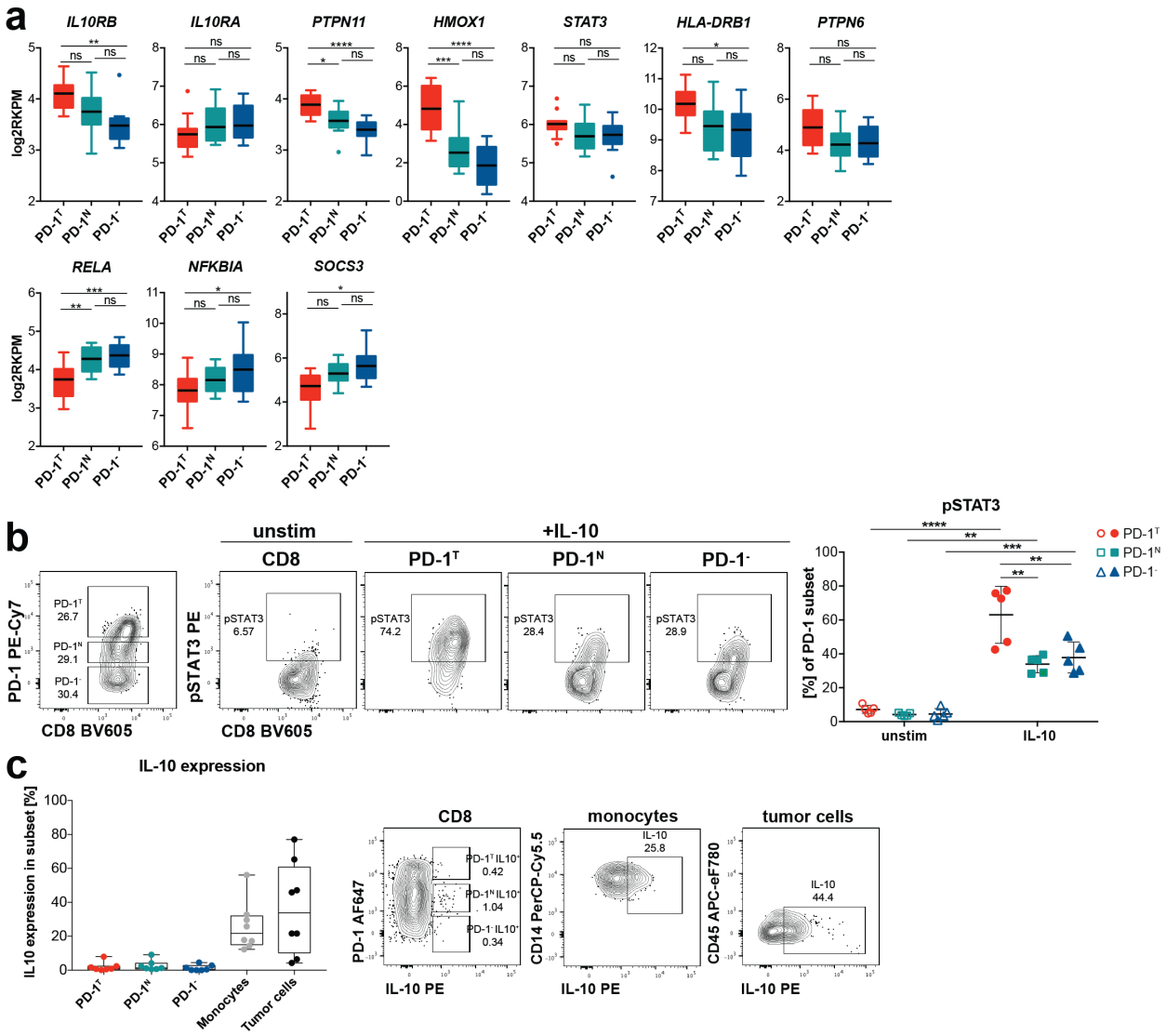

Supplementary Figure 5. IL-10 target genes and IL-10 induced pSTAT3 expression in PD-1 subsets. (**a**) Expression of genes targeted by IL-10 in PD-1^T, PD-1^N and PD-1$^-$ TILs (n=11). The lines in the box-and whisker-plots indicate median values, the boxes IQR values and the whiskers 1.5IQR values as calculated by Tukey. *P < 0.05, **P < 0.01, ***P < 0.001 ****P < 0.0001 by one-way ANOVA. (**b**) IL-10 induced pSTAT3 expression in PD-1^T, PD-1^N and PD-1$^-$ TILs. Shown are the respective flow cytometry plots of one representative donor and the quantification of five donors. Lines and error bars indicate mean and SD. **P < 0.01, ***P < 0.001 ****P < 0.0001 by two-way ANOVA. (**c**) IL-10 expression in PD-1 subsets compared to monocytes and tumor cells (n=8 tumor specimens). Lines in box-and-whisker-plots indicate median values, boxes indicate IQR values and whiskers minimum and maximum values.

Supplementary Figure 6

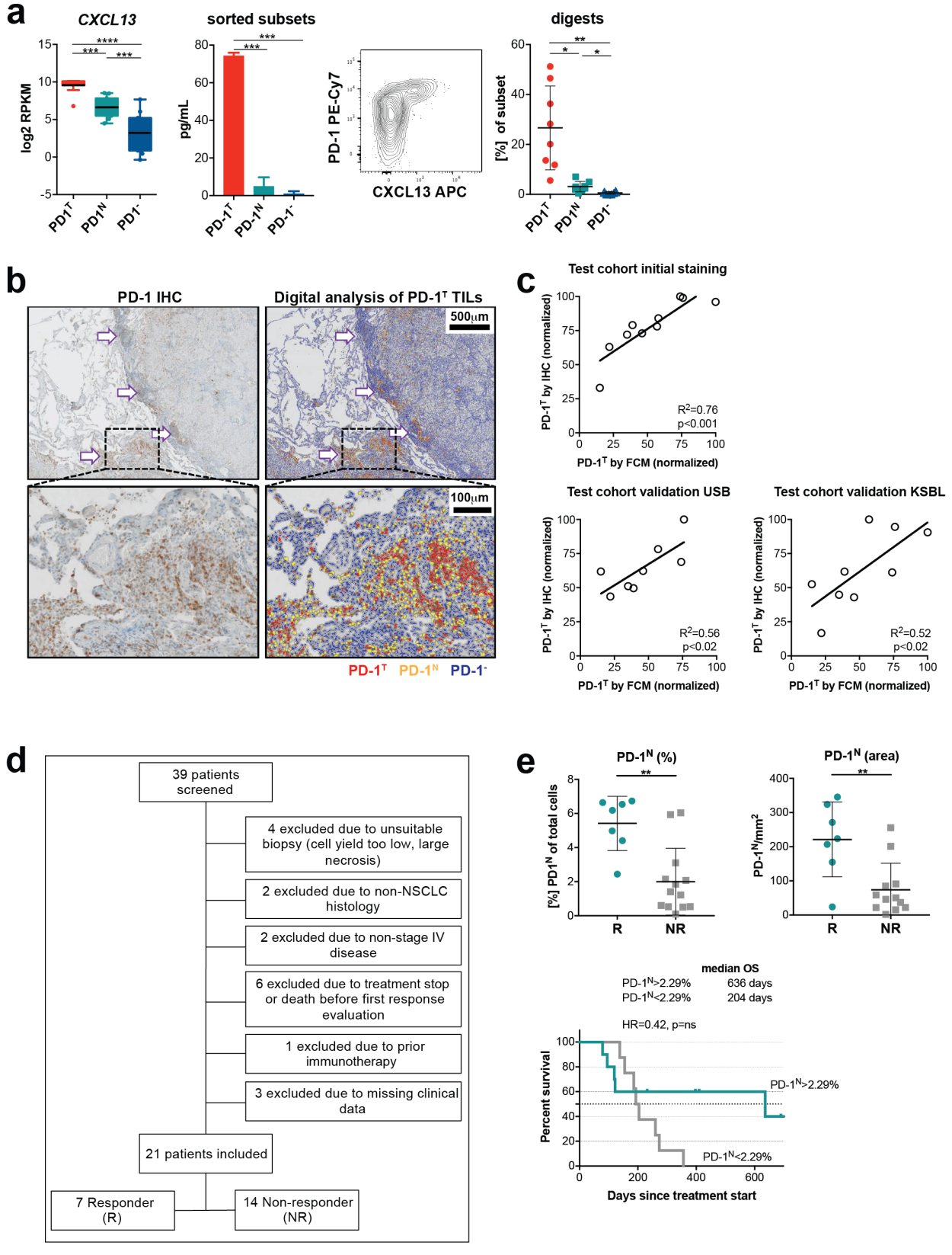

Supplementary Figure 6. CXCL13 expression in PD-1 subsets and development of quantitative PD-1 IHC and study overview. (**a**) CXCL13 RNA expression in sorted PD-1 subsets (left, n=11), CXCL13 protein secretion by sorted PD-1 subsets analyzed by bead-based immunoassay (second from left, n=3), and CXCL13 protein expression analyzed by intracellular cytokine staining of cells with distinct PD-1 levels (second from

right and right, n=8). Box-and whisker-plot: the lines in the indicate median values, the boxes IQR values and the whiskers 1.5IQR values as calculated by Tukey. Bar graph: shown are mean and SD. Dot plot: shown are mean and SD. *P < 0.05, **P < 0.01, ***P < 0.001 ****P < 0.0001 by one-way ANOVA. (**b**) Conventional PD-1 IHC and algorithm-based digital PD-1^T, PD-1^N and PD-1^- annotation. (**c**) Correlation of flow cytometry guided quantification of PD-1^T cells with digital analysis of IHC staining in a test cohort of 10 NSCLC specimens (upper part, n=10). Validation of this analysis strategy at two different Pathology departments (USB and KSBL), in which the automated staining and analysis process was carried out using independent tissue slides from the same tumor specimens (lower part, n=8 and n=9, respectively). R square values were calculated using linear regression analysis. (**d**) Study design for analysis of PD-1^T cells in pretreatment biopsies within a retrospective cohort of stage IV NSCLC patients with no prior immunotherapy that underwent anti-PD-1 treatment. The pathologists carrying out the analysis were blinded to the clinical outcome. (**e**) Percentage of PD-1^N TILs per total cells (upper left part) or number of PD-1^N cells per mm^2 in responders (n=7) and non-responders (n=14) to PD-1 blockade (upper right part). Shown are mean and SD. **P < 0.01 by Mann-Whitney test. Overall survival of patients with tumors harboring more or less than 2.29% of PD-1^N cells (lower part, n=21). P value was determined by log-rank test.